Original papers

Granular Matter 5, 171–175 © Springer-Verlag 2004
DOI 10.1007/s10035-003-0141-y

Effects of scale and inertia on granular banding segregation

A. Alexander, F. J. Muzzio, T. Shinbrot

Abstract We report that the formation of much reported axial segregation bands in rotating cylinders loaded with different sized particles depends critically on scale and inertia. Specifically, when the ratio, δ, of the diameter of the cylinder to the average diameter of the particles is large, axial bands invariably appear, when δ is small, bands never appear, and between these extremes lies a reversible state where the presence or absence of bands depends on container rotation speed. Our results indicate that banding is associated with a Rayleigh-like instability of a granular core of fine particles, and that this instability is controlled by the inertia of the larger species – and consequently on scale.

Keywords Granular, Segregation, Mixing, Banding, Scale

It has long been known that blends of different size particles segregate when agitated [1,2]. In a rotating drum, 'radial' segregation occurs promptly, characterized by small particles forming a core along the axis of rotation and large particles surrounding this core. Subsequently, axial bands (see figure 1) of nearly pure components often form [3]. Reports of axial 'banding' segregation abound in the recent literature, and the topic has garnered much interest both theoretically and experimentally [4–10]. Particularly intriguing has been the work of Hill and Kakalios [10], who identified blends that appear mixed at low rotation speeds but form bands at higher speeds. In that work, it was determined that differences in the dynamic angles of repose (ϕ) of pure versus mixed phases dictated whether or not bands form: when ϕ of the larger species and of the mixed phase are similar, a banded state is suppressed, but when these ϕ values differ, bands appear. In this letter, we confirm the results of Ref. [10], but report that those outcomes represent a subset of a broader picture in which the presence or absence of banding depends crucially on mean particle and container size.

To investigate axial banding in greater breadth, we performed experiments in clear acrylic cylinders of different inner diameters (approximately 2.5, 5, 6, 9.5, 12, and 14.5 cm), all 30 cm in length and rotated at fixed speeds under stepper motor control. In each experiment, a cylinder is filled to 50% of capacity with an equal volume binary mixture of sieved spherical glass beads varying in size from 0.2 mm to 6 mm and dyed to provide visual contrast. We restrict ourselves to mixtures for which the particle size ratio, $\mathbf{\Phi}$, is less than 6.5: above $\mathbf{\Phi} = 6.5$, the interstices between large particles are wide enough to allow spontaneous interparticle percolation [11,12] which, though important, is not part of the present study.

Figure 1 shows the range of phenomena that occur as particle diameters, cylinder diameters and rotation rates are varied. For a given experimental condition (particle sizes, cylinder diameter, and rotation rate) only one outcome prevails, either banded or what has historically been described as 'mixed' (which more precisely is a radially segregated state without bands). As shown in Fig. 1, changes in mean particle size, cylinder size or rotation rate can each significantly alter the mixture behavior.

For a given mixture/cylinder pair, we define three states of segregation behavior:

1. The contents are 'mixed' at both 10 rpm and 30 rpm,
2. The contents are 'mixed' at 10 rpm but are banded at 30 rpm (reversibility),
3. The contents are banded at both rotation rates.

Figure 2 shows our determinations of each of these behaviors in over 100 separate experimental combinations of mixtures and cylinders, alongside the results of Hill and Kakalios [10]. In this figure, we see a consistent trend in which there is a transition from an always banded state through a reversible state to a never banded state as either the average particle size is increased or the cylinder diameter is decreased. These trends are codified in their simplest form by the ratio, $\delta = \mathrm{D}/\mathrm{d}_{avg}$, of cylinder diameter, D, to mean particle diameter, d_{avg}. As indicated by the lines that partition Fig. 2, when δ exceeds about 55, banding segregation always occurs, when it is less than about 40, banding segregation is never seen, and between these values the state is reversible with the presence of banding depending on the cylinder rotation rate. The two rotation rates used in Ref [10] were 5 and 15 rpm (whereas our rotation speeds were 10 and 30 rpm), and the cylinder in Ref. [10] was filled to 33% of capacity (as compared with our experiments using 50% fill). The sizes and speeds used

Received: 16 April 2003

A. Alexander, F. J. Muzzio
Department of Chemical and Biochemical Engineering,
Rutgers University, Piscataway, NJ 08855, USA

T. Shinbrot (✉)
Department of Biomedical Engineering,
Rutgers University, Piscataway, NJ 08855, USA
e-mail: shinbrot@sol.rutgers.edu

PACS number(s): 05.40.+j, 46.10.+z, 83.10.Hh.

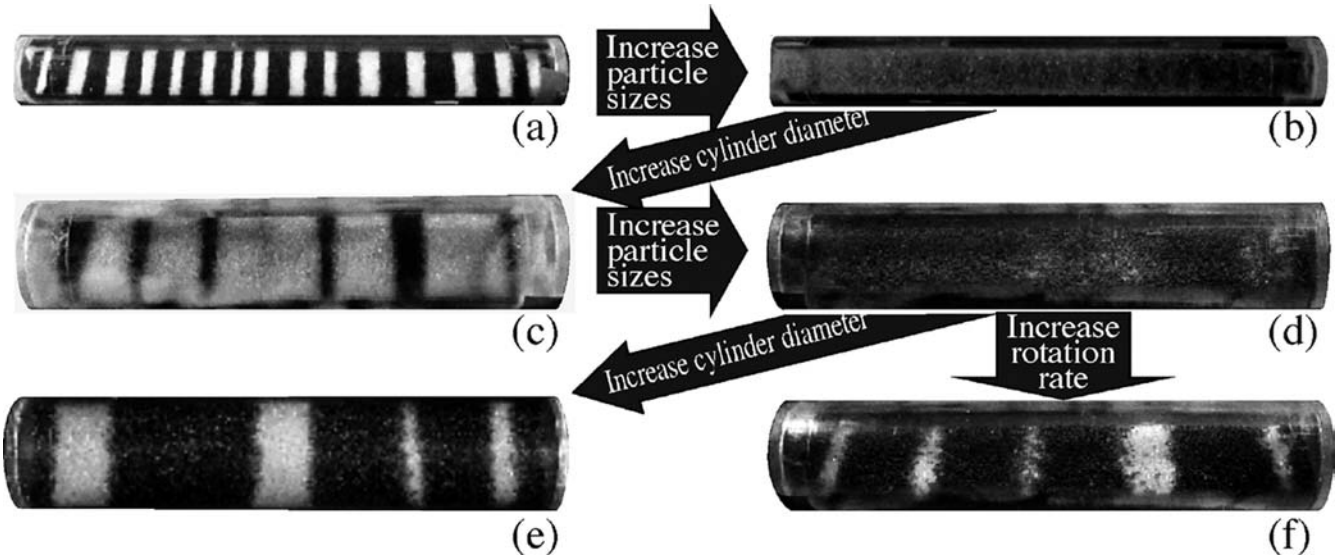

Fig. 1. Experimental outcomes of tumbling experiments using different mean particle sizes and container diameters. In each experiment, an equal volume pre-mixed binary blend of glass beads is loaded into a cylinder that is rotating at constant speed for 20 minutes. In case (a), 0.4 mm and 0.2 mm particles form axial bands when rotated at 10 rpm in a 2 cm diameter cylinder; in (b), increasing the particle sizes to 0.8 mm and 0.4 mm results in a 'mixed' state in the same cylinder; in (c), increasing the cylinder diameter to 5 cm reverts to axial band formation; in (d), increasing particle sizes to 1.6 mm and 0.8 mm once again represses bands; and in (e) and (f) either increasing cylinder size to 6 cm or increasing the rotation rate to 30 rpm restores axial bands. All snapshots are taken after stopping the cylinder, and darker particles are larger in all but snapshot (c)

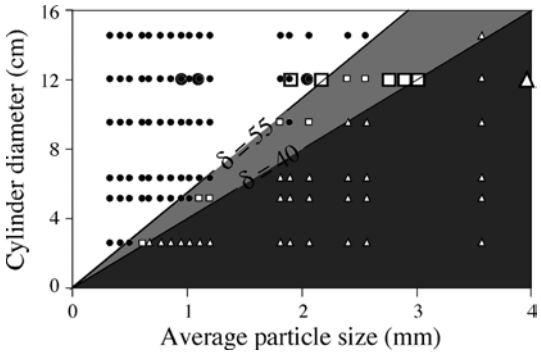

Fig. 2. Banding data as a function of cylinder diameters and average particle size. Each data point represents a separate experiment (circles always band, squares band reversibly depending on rotation speed, and triangles never band). Shaded regions are delineated by the ratio $\delta = \mathrm{D}/\mathrm{d}_{avg} = 40$ and 55 as indicated. Data from Hill and Kakalios [10] are identified by larger symbols

in our study are chosen to provide steady flow for all cylinder and particle combinations, and the ranges of δ for each type of mixture behavior are consequently slightly different between our data and those of Ref [10], however the trend with changes in δ in both studies is as we report.

To understand the cause of the transition between banding and non-banding states, we note that MRI results of Hill et al. [6] and of Nakagawa [13] show that in the banded state, the core alternately swells and narrows along its axis, leading to the proposition [6] that visible bands are best be viewed as an extension to the surface of Rayleigh-like instabilities in the core shape [14]. This instability is well known in fluid mechanical circles, where surface tension in a cylindrical stream of water (e.g. flow from a tap) causes the fluid stream to neck and break into droplets.

We test this proposition in three ways, first by varying the relative concentration of constituent particles, second by altering their density contrast, and third by computationally simulating the core dynamics. For the first test, we observe that the proposition that banding is governed by an underlying Rayleigh-like core instability indicates that in mixtures with fewer large particles, the valleys in the core should be able to absorb a higher fraction of large particles, thus accentuating banding. Contrariwise, mixtures with increased large particle concentrations should inhibit banding. Indeed, in separate experiments we found (1) that non-banding systems (e.g. the 6 cm cylinder charged with the blend of 3 mm and 0.8 mm particles and rotated at 10 rpm) band when the large particle concentration is reduced to 30%, and (2) that banding is suppressed when the large particle concentration is increased to 70% in mixtures that otherwise band (e.g. 1.6 mm and 0.6 mm particles, again in the 6 cm cylinder rotated at 10 rpm).

For the second test, we seek to partially disentangle the mechanism of banding by exploring the extent to which the apparent instability of the core is dominated by large versus small particle dynamics. *A priori*, it seems equally plausible that the core could expand locally due to an intrinsic (yet to be defined) transverse instability of the core itself, or that the core could be locally deformed by the dynamics (also to be clarified) of the larger species. To

provide some insight into this issue, we have performed an additional set of experiments in which we used glass particles coated with a dye that rendered the particles 20% more dense than before. To the best of our observations, the heavier particles do not flow or interact any differently than the lighter particles, and the sole observable difference between the particles is the density of the dye. These experiments were intended to investigate the possibility that by increasing the density, and hence the inertia, of the larger particles we would increase their tendency to displace the core [15], thereby enhancing the development of axial bands. This hypothesis is evaluated by comparing 50-50 blends of 1.6 mm and 0.8 mm particles first with identical density beads and second with 1.6 mm particles that are 20% more dense than the 0.8 mm particles. In these experiments, we found that no bands are apparent when rotated in the 5 cm cylinder at 10 rpm, but when the same experiment is run with the denser 1.6 mm particles, bands do form.

From these two tests, we conclude that available evidence supports the proposition that axial banding is the overt expression of an underlying transverse instability in the radially segregated core formed during granular tumbling. Additionally, two pieces of evidence presented in this letter suggest that this instability is mediated by the inertia of the larger species. First, axial bands appear only when the ratio, δ, of cylinder diameter to average particle size is large (Fig. 2). As δ grows, each particle undergoes more collisions while in the flowing cascade, and thus the number of opportunities for inertia-dominated deformation of the core could be expected to increase with δ. Second, non-banding mixtures tend to band at higher rotation speeds (Fig. 1f), which is associated with greater momentum transfer during collisions. Since, as we have described, large particles predominate at the surface early in the segregation evolution, the tendency to band with increased speed or large particle density indicates that the momentum of the larger species mediates core deformation.

Third, to investigate whether a Raleigh-like core instability of a granular core can be expected from known Physics and to understand the putative instability's role on banding and cylinder scale, we construct a numerical simulation in which we track the interface between the core of fines and the surrounding coarse particles. The approximations intrinsic to tracking only the core interface permits us both to study the interfacial dynamics of interest and to achieve a considerable computational advantage over particle-dynamic or other simulations that attempt to track every particle. To devise the simulation, we observe that what is known of the core instability is as follows.

(1) *The transverse bands form after a well defined, radially segregated, core of fines assembles.* Therefore we begin by defining a uniformly defined set of marker points distributed on the surface of a cylindrical core of mean dimensionless diameter D_c, with random perturbations initially added to their radial positions to mimic granular variability.

(2) *Transport in the rolling regime can be accurately modeled by assuming that material above a shear band flows nearly parallel to the granular free surface, while beneath the band material rotates nearly as a solid body* [13,16,17]. This model, originally applied to tumbling of monodisperse blends, applies also to material in the core of a polydisperse blend – it too must rotate with the cylinder and it too must flow when it exceeds some internal slip angle. The velocities in the core will not in general coincide with those outside, but nevertheless this approximation should (and is experimentally seen through the sidewalls) describe the core flow. Algorithmically, we produce this flow by rotating all interface points steadily counter-clockwise as a solid body at angular speed, ω, and additionally translating points above a fixed 'slip line' parallel to that line. For convenience, we use a Cartesian coordinate system inclined at the angle of repose of the free surface, so that the slip line (i.e. the direction of cascading flow) is in the $\hat{x}$-direction.

(3) *In the cascading layer, flow of coarse particles outside the core is faster than flow of fines inside.* This is observed experimentally [18] in tumbling blenders, and to account for this behavior, we assume that the core interface accelerates in the cascading region whenever the radius exceeds the initial core radius. To generate the acceleration, we add a velocity, $\Delta v \cdot \hat{\mathrm{x}}$, to the velocity of interfacial elements in the forward half of the cascading layer, where $\Delta v = -v\partial\omega\ \mathrm{R}^{\alpha}$. We simplify the acceleration of the core in the cascading layer by only adding this velocity to the forward half of the layer for two reasons: first, the precise nature of this acceleration is not known and is problematic to measure properly, and second this approximate method is computational efficient and simple to program. In the results displayed here we choose $\mathrm{v}_o = \alpha = 2$ to represent the acceleration of smaller core particles by larger, faster moving, particles outside the core. Other values of these coefficients would work as well: in comparison simulations we have found that for significantly smaller v_o or α, banding never appears, however provided v_o and α are sufficiently large to deform the core faster than the interface is normalized and smoothed (described below), a transition between banding and non-banding states is easily observed.

(4) *Fines always return to the core, and so neglecting attrition and dilatency, the mass of fines within the core interface is conserved.* This essentially Archimedean displacement is approximated in our simulation by explicitly conserving *volume* of the core, by two means. *Locally* the simulation volume is normalized by equally increasing (decreasing) the radii of the nearest neighbors of any point whose radius is moved inward (outward) as compared with its prior radial position. This is done so as to uniformly redistribute the volume to exactly compensate for any inward (outward) local displacement. At the two end boundaries of the core, volume is still conserved in the same way, but using 3 instead of 4 nearest neighbors. No other boundary condition is imposed. *Globally*, the simulation is normalized by computing the total, naively integrated, volume enclosed in the discretized interface and increasing or decreasing all radii

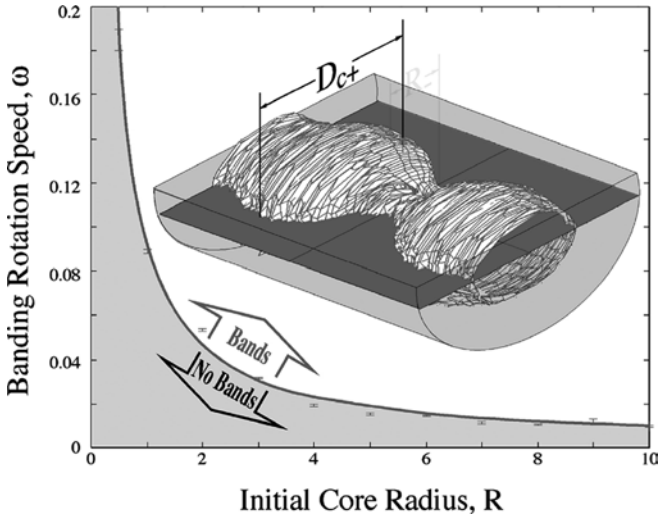

Fig. 3. Onset of banding seen in simulation modeling core interface described in text. Above the onset curve, $\omega \cdot R^{1.03} = 0.09 \cdot$ ($r^2 = 0.988$) banding is reproducibly seen, below it banding does not develop. Error bars on data points are the *range* of data from multiple computational trials: above the upper error bar, banding always occurs and below the lower bar it is never seen. Inset shows a typical banded outcome state: banding is determined to occur if the maximum diameter, D_{c+} exceeds twice the mean diameter, D_c. The gray plane indicates the shear plane below which the core only rotates as a solid body; above this plane the core rotates *and* translates as described in text

at every gridpoint by the same factor so as to maintain the global volume constant. Effectively, the local and global volumetric compensations act to redistribute the core interface so that when a region is pushed inward, neighbors move outward and the core as a whole expands to maintain a fixed total core volume. This is done 'naively', meaning in proportion to the radius alone, neglecting curvatures, proximities of neighbors, etc. using the approximation, Volume = $\Sigma[R_{ij^2}\Delta\vartheta\Delta\ z/2]$, where R_{ij} are the interfacial radii at location ϑ_i, z_j, and $\Delta\vartheta$ and Δz are the initial azimuthal and axial marker separations.

Finally, the surface is smoothed by averaging every grid point radius over its 5 nearest neighbors in the simplest possible manner: this is not essential, but it limits the amplitudes of small wavelength fluctuations.

The simulation that tracks the core interface (available at http://coewww.rutgers.edu/∼shinbrot/Banding/index.html) produces a transverse banding instability with a transition that parallels that seen in our experiments. Results in the banding state are summarized in Fig. 3. In the inset, a typical simulation outcome is shown: here the curved surface is the core interface after 100 computational time units with parameter values as indicated in the figure caption. The dark plane indicates the slip plane above which the interface gains an additional velocity as described above.

In the main figure, we plot the onset of banding: above the curve shown, banding is reproducibly seen and below it banding is absent. Bands are determined to occur if the largest diameter (D_{c+} in the inset) reaches twice the initial cylindrical core diameter after a fixed amount of time (the same 100 time units whose outcome is shown in the inset). Qualitatively, this curve agrees with the results described in Fig. 1: at small scales and low rotation speeds, banding is suppressed, while increasing the speed or the scale reproducibly produces banding.

The underlying assumption here is that banding is the overt expression of sufficiently large Rayleigh-like bands, and in this interface tracking model the banding instability is generated by a competition between acceleration of the topmost core particles by faster moving coarse particles and the assumed conservation of the total core volume. Effectively, small bulges in the core interface get stretched by the acceleration imposed by observation (3) above each time they visit the cascading surface. As the bulges grow, material to fill the bulges comes from nearby regions of the core, according to observation (4). In this way, accompanying each bulge is a nearby valley, and the cascading flow stretches both bulges and valleys around the circumference of the core to produce the observed bands.

Experimentally, the growth of bands is limited by dispersion, so that when the rate of growth of bulges (due to acceleration by faster moving particles) exceeds the rate of dispersion (due to outward propagation of disturbances required by volume conservation), then the bulges can grow until they emerge at the surface as bands. The rate of growth of a radial disturbance is $\Delta v = -v_o \omega\ D_C^{\alpha}$, while the speed of dispersion due to volume conservation is $U = d/\tau$, where d and τ are the computational grid spacing and timestep respectively. Taking $d = \pi D_C/N$ for N markers per core circumference, we obtain the estimate that onset of banding should occur when $|\ \Delta v\ | > U$, or $\omega D_C^{\alpha-1} > 2\pi\ /N\tau\ v_o$. Since our simulations use $\alpha = 2$, we obtain an expected $\omega\ D_C$ = constant onset curve, which is to be compared with the best fit to the data shown in Figure 3: $\omega \cdot R^{1.03} = 0.09$. Note that this quantitative transition curve is based on the choice of α. This choice in turn is nearly arbitrary, as it merely defines a rate of acceleration with radius – provided that this acceleration is sufficient to overcome dispersive smoothing, bands will inevitably emerge. Therefore there is no reason to expect banding onset to be quantitatively governed by this particular simple onset equation; however the qualitative onset behavior displayed in Fig. 3 should hold provided that $v_o \omega \tau D_C^{\alpha-1} \gg 1$.

This model tells us three things then. First, non-banding cores can be made to band if the rotation speed, ω, or the system size, D_C, is increased sufficiently. This prediction is bounded by the applicability of the assumptions made: in particular they apply in the rolling regime where the cylinder free surface is nearly flat. Second, the core diameter, D_C, is assumed to be dimensionless, and the nature of the competition leading to the instability suggests that the relevant scale size – indeed the only distance scale present – by which D_C should be nondimensionalized is d, the micro-scale dimension at which dispersion takes place. It seems reasonable to set $D_c \sim D$ and $d \sim d_{avg}$, and in this case the simulation accords with

the experimental finding that the scale of banding onset should be set by the ratio, δ, of cylinder (or core) size to particle (or dispersion) length. Third, the simulation reveals a hitherto unreported finding deserving of more careful experimental scrutiny. That is, because the Rayleigh-like instability is generated by a growth of bulges, in simulations far from onset, banding is often preceded by an azimuthally asymmetric bulge that eventually disperses around the core circumference. This asymmetry should be experimentally observable as intermittent protrusions of the core to the surface in axial locations where bands subsequently develop.

In conclusion, although the prevailing model for axial band development emphasizes differences in the dynamic angle of repose (ϕ) with variations in axial particle concentrations, it seems important to stress that these differences can arise only *after* radial concentration variations have *already* brought small particles back to the surface following radial segregation. A complete understanding of the evolution and mechanism of band formation thus demands more comprehensive study in the future of the initiation and nature of the Rayleigh-like instability of the radially segregated core. Our results suggest two lessons in this respect. First, this instability seems to be most strongly controlled by inertially-dominated deformation of the core by the larger species; this is not the only conceivable explanation for the effects seen, but it seems consistent with the available data. Second, more broadly speaking, our results underscore the importance of considerations of scale in granular studies. Unlike simple fluids, granular dynamics are not conducive to description using scale-invariant dimensionless groups analogous, for example, to Reynolds or Taylor numbers, and consequently the implications and mechanisms underlying granular dynamics seem unlikely to be fully understood in the future without careful analysis of consequences of scale.

References

1. Y. Oyama, Bull. Inst. Phys. Chem. Res. (Tokyo) Rep. 5, 600 (1939), p. 1962
2. M. B. Donald & B. Roseman, Brit. Chem. Eng. 7 (1962), p. 749–53
3. S. D. Gupta, D. V. Khakhar & S. K. Bhatia, Chem. Eng. Sci. 46 (1991), p. 1513–8
4. T. Elperin & A. Vikhansky, Phys. Rev. E. 60 (1999), p. 1946–50
5. K. M. Hill, A. Caprihan & J. Kakalios, Phys. Rev. E. 56 (1997), p. 4386–93
6. K. M. Hill, A. Caprihan & J. Kakalios, Phys. Rev. Lett. 78 (1997), p. 50–3
7. D. Levine, Chaos. 9 (1999), p. 473–80
8. L. Prigozhin & H. Kalman, Phys. Rev. E. 57 (1998), p. 2073–80
9. J. Stavans, J. Stat. Phys. 93 (1998), p. 467–75
10. K. M. Hill & J. Kakalios, Phys. Rev. E. 52 (1995), p. 4393–400
11. J. Bridgwater, Trans. Instn. Chem. Engrs. 49 (1971), p. 163–9
12. A. M. Scott & J. Bridgewater, Ind. Eng. Chem. 14 (1975), p. 22–7
13. N. Nakagawa, S. A. Altobelli, A. Caprihan & E. Fukushima, Chem. Eng. Sci. 52 (1997), p. 4423–8
14. W. K. Lee & R. W. Flumerfelt, Int. J. Multiphase Flow 7 (1981), p. 363–81
15. A. W. Alexander, T. Shinbrot & F. J. Muzzio, Phys. Fluids. 13 (2001), p. 578–87
16. D. V. Khakhar, J. J. McCarthy, T. Shinbrot & J. M. Ottino, Phys. Fluids 9 (1997), p. 31–43
17. J. M. N. T. Gray, J. Fluid Mech. 441 (2001), p. 1–29
18. A. W. Alexander, T Shinbrot & F. J. Muzzio, Phys. Fluids A 13 (2001), p. 578–87